



You have downloaded a document from  
**RE-BUŚ**  
repository of the University of Silesia in Katowice

**Title:** EPID-a useful interfraction QC tool

**Author:** Aleksandra Klimas, Aleksandra Grządziel, Dominika Płaza, Barbara Bekman, Bożena Woźniak, Łukasz Dolla, Wojciech Osewski, Paweł Paściak, Jacek Wendykier, Krzysztof Ślosarek

**Citation style:** Klimas Aleksandra, Grządziel Aleksandra, Płaza Dominika, Bekman Barbara, Woźniak Bożena, Dolla Łukasz, Osewski Wojciech, Paściak Paweł, Wendykier Jacek, Ślosarek Krzysztof. (2019). EPID-a useful interfraction QC tool. "Polish Journal of Medical Physics and Engineering" (Vol. 25, nr 4 (2019), s. 1-8), doi: 10.2478/pjmpe-2019-0029



Uznanie autorstwa - Użycie niekomercyjne - Bez utworów zależnych Polska - Licencja ta zezwala na rozpowszechnianie, przedstawianie i wykonywanie utworu jedynie w celach niekomercyjnych oraz pod warunkiem zachowania go w oryginalnej postaci (nie tworzenia utworów zależnych).



Scientific Paper

## EPID – a useful interfraction QC tool

Aleksandra KLIMAS<sup>1,2</sup>, Aleksandra GRZĄDZIEL<sup>3</sup>, Dominika PLAZA<sup>3</sup>, Barbara BEKMAN<sup>3</sup>, Bożena WOŹNIAK<sup>4</sup>, Łukasz DOLLA<sup>3</sup>, Wojciech OSEWSKI<sup>5</sup>, Paweł PAŚCIAK<sup>3</sup>, Jacek WENDYKIER<sup>3,a</sup>, Krzysztof ŚLOSAREK<sup>3</sup>

<sup>1</sup>Medical Physics Department, Zagłębiowskie Oncology Center, Dąbrowa Górnicza, Poland

<sup>2</sup>Medical Physics Department, Institute of Physics, University of Silesia, Chorzów, Poland

<sup>3</sup>Radiotherapy Planning Department, Maria Skłodowska-Curie Institute – Oncology Center Gliwice Branch, Gliwice, Poland

<sup>4</sup>Medical Physics Department, Maria Skłodowska-Curie Institute – Oncology Center Gliwice Branch, Gliwice, Poland

<sup>5</sup>IT Department, Maria Skłodowska-Curie Institute – Oncology Center Gliwice Branch, Gliwice, Poland

<sup>a</sup>jacek.wendykier@io.gliwice.pl

(received 21 November 2019; revised 3 December 2019; accepted 4 December 2019)

### Abstract

Biomedical accelerators used in radiotherapy are equipped with detector arrays which are commonly used to obtain the image of patient position during the treatment session. These devices use both kilovolt and megavolt x-ray beams. The advantage of EPID (Electronic Portal Imaging Device) megavolt panels is the correlation of the measured signal with the calibrated dose. The EPID gives a possibility to verify delivered dose. The aim of the study is to answer the question whether EPID can be useful as a tool for interfraction QC (quality control) of dose and geometry repeatability.

The EPID system has been calibrated according to the manufacturer's recommendations to obtain a signal and dose values correlation. Initially, the uncertainty of the EPID matrix measurement was estimated. According to that, the detecting sensitivity of two parameters was checked: discrepancies between the planned and measured dose and field geometry variance. Moreover, the linearity of measured signal-dose function was evaluated.

In the second part of the work, an analysis of several dose distributions was performed. In this study, the analysis of clinical cases was limited to stereotactic dynamic radiotherapy. Fluence maps were obtained as a result of the dose distribution measurements with the EPID during treatment sessions. The compatibility of fluence maps was analyzed using the gamma index. The fluence map acquired during the first fraction was the reference one. The obtained results show that EPID system can be used for interfraction control of dose and geometry repeatability.

**Key words:** EPID; gamma index; fluence map.

### Introduction

Electronic portal devices were proposed for clinical practice at the turn of the 20<sup>th</sup> and 21<sup>st</sup> centuries. They were dedicated for the verification of patient setup during the therapeutic session [1,2], as well as for the dose estimation [3-8]. Initially, only a megavolt beam was used both for planar images and volumetric reconstructions CBCT (Cone Beam Computed Tomography). The advantage for CBCT reconstructions is the minimized amount of artifacts from metal objects, compared to the number of artifacts obtained with the use of kilovolt beam. The disadvantages are the worse tissue differentiation and the higher dose delivered to the patient during imaging while comparing with kilovolt beams [9]. In addition, dedicated software was developed to reduce the metal artifacts in acquired images that are produced by high-density materials [10-12]. Till now, this kind of software is available only for computed tomography scanners (CT). It is highly probable that

this type of software will be implemented for OBI (On-Board Imaging with kilovolt x-ray beam), which is used in IGRT (Image Guided Radiation Therapy) techniques. Thus, the question appears if megavolt detectors integrated with the therapeutic units still have a future. Certainly, those detectors can be used for dose measurement during the therapeutic sessions. EPID is commonly used to compare the calculated and measured fluence map. It should be noted that such verification procedures are usually done with a patient's absence and are a part of dynamic plans QA [13,14]. Such measurements do not give the information on dose distribution in patient body. The reconstruction of patient dose absorbed in a single fraction requires dedicated software [15-21]. The proposed proceeding would allow correlating the EPID signal collected during the irradiation with the dose in patient body. This would enable EPID dosimetry without new software and hardware usage.

## Material and method

The study was performed with aS1200 EPID devices integrated with TrueBeam and Edge accelerators (Varian Medical Systems, Palo Alto, CA, USA). The active panel area is  $43.0 \times 43.0 \text{ cm}^2$ , with a resolution of  $1280 \times 1280$  pixels and with a maximum recording speed of 20 sets of frames per second [22]. During the acceptance tests and commissioning measurements, all EPID matrices were calibrated following the manufacturer's recommended procedures [23].

### Phantom set-up

In all measurements, the tissue-like phantom EASY CUBE Body Module S (Lap GmbH Laser Applikationen, Lueneburg, Germany) was used. Additionally, culture flask (Falcon,  $25 \text{ cm}^2$ , <https://en.vwr.com>) was filled with water and placed inside the EASY CUBE phantom. Their location can be clearly visible in both kilovolt and megavolt imaging (**Figure 1**). First, the phantom CT imaging was performed using data acquisition and image reconstruction protocols as used clinically for typical head scans. Imaging data were imported into the Eclipse v.13.6 TPS (Treatment Planning System) (Varian Medical Systems, Palo Alto, CA, USA), and the treatment plan was created.

### Plan preparation

The treatment field was set up to  $15 \times 15 \text{ cm}^2$  at the isocenter located on the flask base. For all photon energies X-6 MV, X-15 MV and X-10 MV-FFF the dose distributions were made with 0.5, 1.0, 2.0 and 7.0 Gy dose specified at isocenter. For the filtered and filtered free beams, the dose rate of 600 MU/min and 2400 MU/min were used respectively. Additionally, for all treatment plans the dose at isocenter was measured with 30013 Farmer ionization chamber and T10001 UNIDOS electrometer (PTW-Freiburg, Germany).

## EPID method sensitivity

The repeatability of the EPID measurements was checked by irradiating four times the EPID matrix for all the mentioned energies and doses. Fluence maps of the  $15 \times 15 \text{ cm}^2$  of the field were acquired in the "Integrated Image" measurement mode [23,24]. For the further analysis a  $2 \times 2 \text{ cm}^2$  region of interest with its center at the isocenter was selected. The agreement of the four measured fluence maps was assessed in the area of interest. The first fluence map was the reference one. The evaluation was conducted with the usage of the gamma index, calculated with the criteria of  $\Delta d = 0.5\%$  and  $\text{DTA} = 0.5 \text{ mm}$  [25].

Four fluence maps acquired for given energy and dose were the independent group of data. Further, those data were the base for the nonparametric tests.

### Linearity

In the region of interest, the mean value of the acquired signals was calculated. The unit of the calculated and measured fluence maps in Varian system is CU (Calibration Units) [24]. The linearity between the number of CU and the dose was checked for all selected beams. Four arbitrary dose values were chosen: 0.5, 1.0, 2.0 and 7.0 Gy.

### Dose and geometry change sensitivity

For the X-6 MV beam, the sensitivity for the dose changes was tested. The doses of 0.45, 0.50 and 0.55 Gy at the isocenter for  $15 \times 15 \text{ cm}^2$  field were prescribed. For these doses the fluence maps were acquired. To assess the differences between the fluence maps of the three doses the gamma index in the area of  $2 \times 2 \text{ cm}^2$  was calculated. Three pairs of gamma criteria were established: (i)  $\Delta d = 0.5\%$  and  $\text{DTA} = 0.5 \text{ mm}$ , (ii)  $\Delta d = 2.0\%$  and  $\text{DTA} = 2.0 \text{ mm}$ , and (iii)  $\Delta d = 4.0\%$  and  $\text{DTA} = 4.0 \text{ mm}$ . To determine the statistical significance the nonparametric tests method for independent samples (Mann-Whitney U test) was performed.

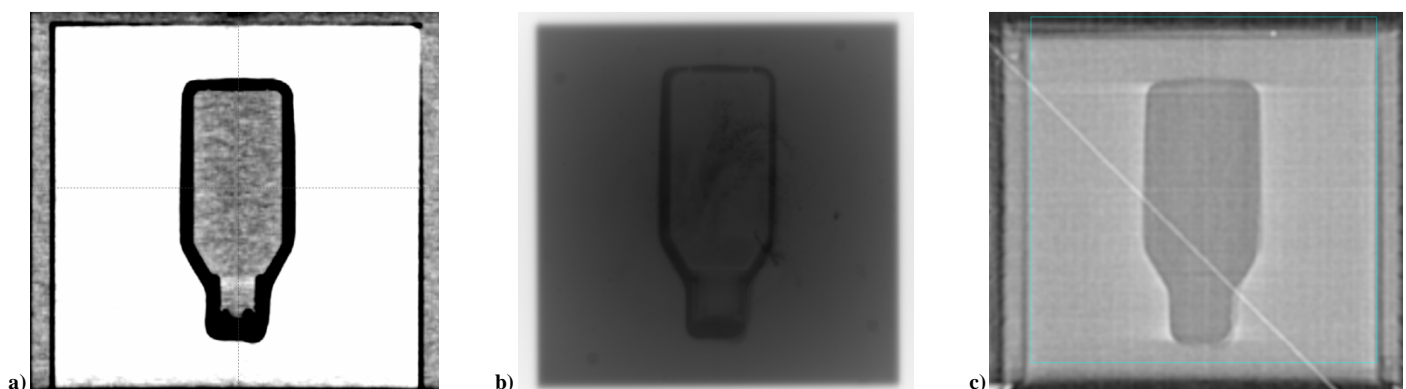


**Figure 1. Imaging of the culture flasks in different x-ray beams: kilovoltage (a), megavoltage (b) and digital reconstruction (DRR) obtained from kilovoltage computed tomography (c).**

**Table 1. Percentage values of the analyzed field that meet the  $\gamma \leq 1$  criteria of  $\Delta d = 0.5\%$  and  $DTA = 0.5$  mm, mean values of CU, standard deviation and uncertainty (bold) calculated for three beam energies and four tested doses.**

Beam	0.5 Gy				1.0 Gy				2.0 Gy				7.0 Gy			
	%S	CU (mean)	SD (CU)	$\Delta$ [%]	%S	CU (mean)	SD (CU)	$\Delta$ [%]	%S	CU (mean)	SD (CU)	$\Delta$ [%]	%S	CU (mean)	SD (CU)	$\Delta$ [%]
X-6MV	98.9	0.103	0.007	<b>7.3</b>	100.0	0.204	0.005	<b>2.7</b>	100.0	0.406	0.002	<b>0.5</b>	100.0	1.430	0.007	<b>0.5</b>
X-15MV	98.9	0.132	0.000	<b>0.2</b>	99.2	0.265	0.001	<b>0.3</b>	99.3	0.531	0.001	<b>0.2</b>	99.3	1.861	0.004	<b>0.2</b>
FFF-X-10MV	99.7	0.129	0.001	<b>0.4</b>	99.8	0.258	0.001	<b>0.4</b>	99.8	0.517	0.002	<b>0.4</b>	99.8	1.812	0.007	<b>0.4</b>

Once more the X-6 MV beam and isocentric  $15 \times 15$  cm<sup>2</sup> field were used for geometry tests. In order to estimate the ability to find a geometric error, the phantom was shifted in the lateral and longitudinal axes by 3.0 mm. The phantom in reference and the shifted position was irradiated and the fluence maps were acquired. Differences between the proper and shifted fluence maps were evaluated with the gamma index in  $2 \times 2$  cm<sup>2</sup> area within four pairs of criteria: (i)  $\Delta d = 0.5\%$  and  $DTA = 0.5$  mm, (ii)  $\Delta d = 2.0\%$  and  $DTA = 2.0$  mm, (iii)  $\Delta d = 4.0\%$  and  $DTA = 4.0$  mm and (iv)  $\Delta d = 5.0\%$  and  $DTA = 5.0$  mm.

Then, the received data were statistically analyzed using nonparametric tests for independent samples. Results of the dosimetric and geometric tests were the base of the null hypothesis stated. The numerical values of fluence maps were the analyzed data sets. There were 8 pairs of sets for different dosimetric and geometrical conditions. The null hypothesis stated: if at least 98% of the analyzed field meets the  $\gamma \leq 1$  condition for  $\Delta d = 2.0\%$  and  $DTA = 2.0$  mm criteria, then the sets are not identical.

### Analysis of clinical cases

The practical usefulness of the EPID matrix as dosimetry system was proved by measurements of the fluence maps. The fluence maps were acquired for 19 fractionated stereotactic plans (VMAT or IMRT). Two measurements were made for 16 patients and three measurements were made for 3 patients. In total, 75 fluence maps were compared and analyzed. For all 87 comparisons were done. Each treatment was realized with the EPID device in mode enabling the measurement of radiation passing through the patient body. The first measured fluence map was the reference one. The next fraction maps were compared to the first one. The gamma index was determined in two ways for (i)  $\Delta d = 0.5\%$  and  $DTA = 0.5$  mm, (ii)  $\Delta d = 2.0\%$  and  $DTA = 2.0$  mm. For both sets of criteria the mean values of gamma index were calculated.

Moreover, each measured fluence map was exported to Statistica v. 12 (<https://www.statsoft.pl>) and using Mann-Whitney U test the comparison was made to check whether these sets are identical. The significance criterion was p-value  $< 0.05$ . This way the similarity of fluence maps for given fields was checked.

## Results

### EPID method sensitivity

**Table 1** shows the percentage of the analyzed field with the gamma coefficient less or equal than one for the criteria:  $\Delta d = 0.5\%$  and  $DTA = 0.5$  mm and the average values of the CU from the area of interest defined as  $2.0 \times 2.0$  cm<sup>2</sup> with the value of the standard deviation. For every energy and dose used in the study, the values of percentage uncertainty ( $\Delta$ ) were calculated. The mean value of the %S calculated for all energy and doses equals 99.1% with the average measurement uncertainty of 1.1%. This value was obtained as the average value of all uncertainties (bold numbers in **Table 1**).

The results of nonparametric tests for independent groups of data showed no statistically significant differences. However, it should be noted that for low energies and doses the measurement uncertainty is greater.

### Linearity

The graph of a signal measured by the EPID matrix during irradiation as the function of the dose for photon radiation: X-6 MV, X-15 MV, and X-10 MV-FFF is shown in **Figure 2**. The correlation coefficient  $R^2 = 0.9999$  shows a linear dependency of the CU value and the dose value. Performed measurements and calculations confirmed strong linear dependency between the dose and the detector signal, which allows using this device to assess radiation doses.

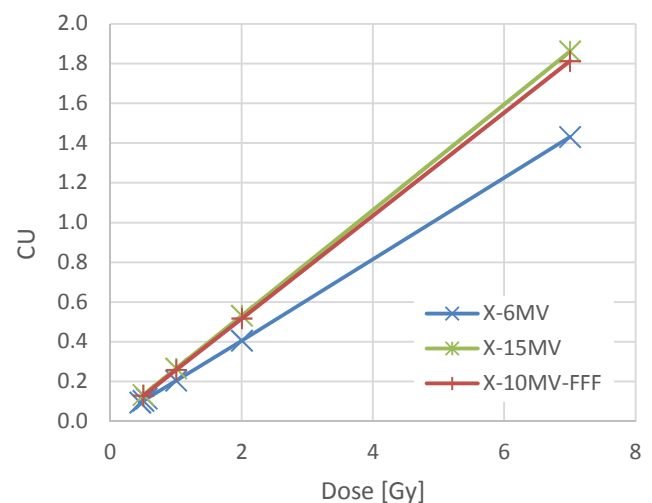


**Figure 2. The measured signal as a function of the dose in the range from 0.5 to 7.0 Gy for photon beams: X-6 MV and X-15 MV and X-10 MV-FFF.**

### Dose and geometry change sensitivity

To evaluate the dose change sensitivity the CU numbers in  $2.0 \times 2.0 \text{ cm}^2$  central area for 0.50 Gy, 0.45 Gy and 0.55 Gy were used. Differences between pairs of fluence maps were calculated using the gamma index. The analyzed data show a significant statistical difference. The results for three different pairs of criteria are presented in **Table 2**. The tested 10% difference of dose significantly affects the %S that meets the criterion of the gamma index for and  $\Delta d = 0.5\%$  and  $\text{DTA} = 0.5 \text{ mm}$ . For assumed criteria, less than 10% of the analyzed area meets the condition of gamma value  $\leq 1$ . On this basis, one can state that a change in dose by 10% can be confirmed by measurements made with EPID matrix. Results indicate that the EPID detector is able to assess the value of delivered dose.

To find a geometric error using fluence map measurement, the 3.0 mm phantom shifts were applied. **Table 3** presents the differences between shifted and non-shifted fluence maps

calculated with four different gamma criteria. Pairs of fluence maps were acquired for three dose values. The results of geometry change analysis show that for 0.5% and 0.5 mm criterion only 78% of the analyzed field meets the acceptance conditions. Therefore, it can be said that a 3.0 mm shift of the phantom causes the differences in the analyzed signal sets. The results were confirmed by statistical tests.

**Table 4** presents the results of comparison of measured fluence maps acquired for three different dose values and two field geometries. Also the calculation of p-value for the Pearson  $\chi^2$  and  $\chi^2$  NW tests is included. The performed tests authorize the rejection of the null hypothesis (Pearson's  $\chi^2$ :  $p = 0.00468$ ;  $\chi^2$  NW:  $p = 0.00114$ ), and therefore one can say that these conditions are dependent. It means that, when the dose differences between measured fluence maps are less than 2.0% and 2.0 mm for 98% of the analyzed field, then the maps are identical and there is an agreement between those measurements.

**Table 2.** The percentage value of the surface of the analyzed field (%S) with gamma index  $\leq 1$  for given pairs of doses and different gamma criteria.

Dose [Gy]	%S gamma $\leq 1$			p-value
	$\Delta d[\%]/\text{DTA}[\text{mm}]$	$\Delta d[\%]/\text{DTA}[\text{mm}]$	$\Delta d[\%]/\text{DTA}[\text{mm}]$	
	0.5/0.5	2.0/2.0	4.0/4.0	
0.45 vs. 0.50	7.6	26.6	31.9	0.000
0.45 vs. 0.55	2.5	24.4	32.2	0.000
0.50 vs. 0.55	8.1	27.1	35.1	0.000

**Table 3.** The percentage value of the surface of the analyzed field (%S) with gamma index  $\leq 1$  for given doses and different gamma criteria for field shift = 3.0 mm.

Dose [Gy]	%S gamma $\leq 1$				p-value
	$\Delta d[\%]/\text{DTA}[\text{mm}]$	$\Delta d[\%]/\text{DTA}[\text{mm}]$	$\Delta d[\%]/\text{DTA}[\text{mm}]$	$\Delta d[\%]/\text{DTA}[\text{mm}]$	
	0.5/0.5	2.0/2.0	4.0/4.0	5.0/5.0	
0.45	75.4	92.0	98.2	99.2	0.000
0.50	78.6	91.8	98.3	99.2	0.000
0.55	78.7	91.2	98.3	99.4	0.000

**Table 4.** The percentage value of the surface of the analyzed field (%S) with gamma index  $\leq 1$  for given doses and shifts for different gamma criteria and results of nonparametric tests.

Shift	Dose [Gy]	%S gamma $\leq 1$			p-value	gamma $\leq 1$ for 98.0% of field (2.0%/2.0mm)	Identical fluence maps
		$\Delta d[\%]/\text{DTA}[\text{mm}]$	$\Delta d[\%]/\text{DTA}[\text{mm}]$	$\Delta d[\%]/\text{DTA}[\text{mm}]$			
		0.5/0.5	2.0/2.0	4.0/4.0			
N	0.50	100.0	100.0	100.0	0.626	Y	Y
Y	0.50	78.6	91.8	98.3	0.000	N	N
N	0.45/0.50	7.6	26.6	31.9	0.000	N	N
Y	0.55	78.7	91.2	98.3	0.000	N	N
N	0.55	100.0	100.0	100.0	0.091	Y	Y
N	0.45/0.55	2.5	24.4	32.2	0.000	N	N
N	0.50/0.55	8.1	27.1	32.4	0.000	N	N
N	0.45	100.0	100.0	100.0	0.464	Y	Y

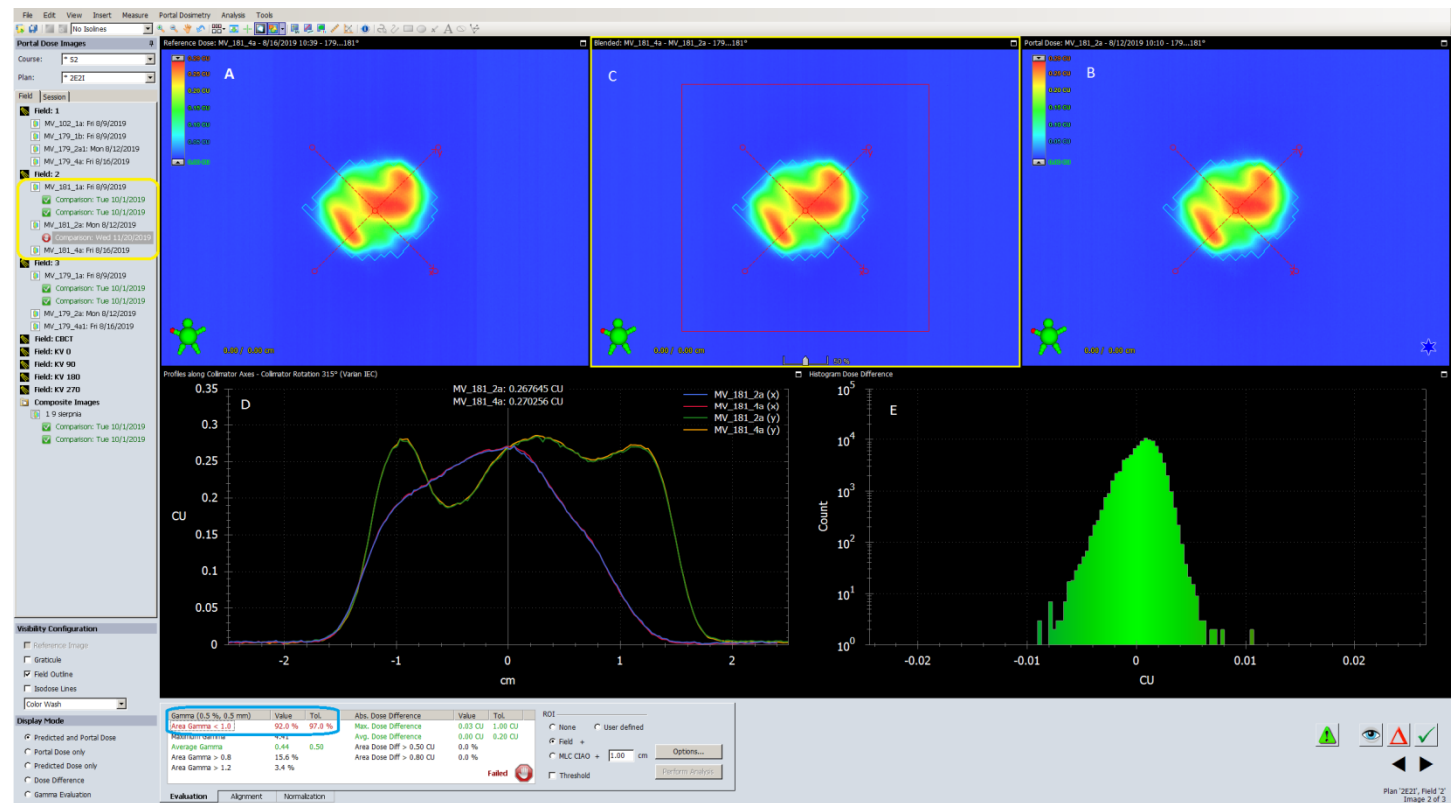


**Figure 3.** Gamma index analysis for an example patient for Field 2. The yellow selection presents acceptable results for  $\Delta d = 2.0\%$  and  $DTA = 2.0$  mm and rejected one for  $\Delta d = 0.5\%$  and  $DTA = 0.5$  mm. The blue selection presents 92.0% of analyzed area that meets the gamma criteria  $\Delta d = 0.5\%$  and  $DTA = 0.5$  mm. Graphics show: (A) first fraction fluence map, (B) second fraction fluence map, (C) blended, (D) profiles along the collimator axes, (E) histogram of dose difference.

## Analysis of clinical cases

**Figure 3** shows example patient results of gamma index calculation for the comparison of two fractions. It is shown, that 92% of the analyzed area meets the gamma index  $\leq 1$  for the criteria of  $\Delta d = 0.5\%$  and  $DTA = 0.5$  mm. However, the change in  $DTA$  value to 2.0 mm and  $\Delta d$  value to 2.0% caused that 100% of the analyzed area meets the gamma  $\leq 1$  condition.

In the case, Mann-Whitney U statistics show that for Field 2 p-value is equal to 0.9440, which means that there is no significant statistical difference between two fluence maps. Therefore, one can conclude that the patient was irradiated with Field 2 repeatedly these days.

All the plans were analyzed the same way what gives 87 comparisons of measured fluence maps. Results of patient-specific measurements present the values of the gamma index showing similarity of fluence maps measured during subsequent therapeutic sessions. The maps were compared each other using two criteria: (i)  $\Delta d = 0.5\%$  and  $DTA = 0.5$  mm and (ii)  $\Delta d = 2.0\%$  and  $DTA = 2.0$  mm. The second evaluation of the identity of the maps was the Mann-Whitney U test. The results are shown in **Table 5**. If gamma index  $\leq 1$  for at least

98% of the analyzed area with criteria of  $\Delta d = 2.0\%$  and  $DTA = 2.0$  mm, then two sets can be considered as identical. This condition is fulfilled in 73 out of 87 analyzed cases.

## Discussion

Dynamic radiotherapy techniques (VMAT and IMRT) require pre-treatment dosimetry verification. The measurement of the fluence map only allows checking if the calculated collimator leaf motion, linac gantry movement, dose rate changes, etc. can be properly realized. It can be also a kind of absolute dosimetry after fulfilling several conditions. For calibration purposes, simultaneous measurements with an ionization chamber and the EPID matrix are necessary. It allows correlating the dose in a phantom with the EPID signal. Also dose distribution from the patient plan has to be converted to the phantom with ionization chamber [26,27]. But it is still not in-vivo dosimetry. The another QA procedure is patient set-up control. The present workflow usually separates the dosimetric verification and patient position check.

Table 5. Results of patient-specific measurements and Mann-Whitney U test.

# patient	%S gamma ≤ 1		p-value	# patient	%S gamma ≤ 1		p-value
	$\Delta d[\%]/DTA[mm]$	$\Delta d[\%]/DTA[mm]$			$\Delta d[\%]/DTA[mm]$	$\Delta d[\%]/DTA[mm]$	
	0.5/0.5	2.0/2.0			0.5/0.5	2.0/2.0	
<b>1 (2 fx)</b>				<b>11 (2 fx)</b>			
field_1	51.7	100.0	0.888	field_1	88.9	100.0	0.890
field_2	62.1	100.0	0.871	field_2	91.6	100.0	0.890
field_3	78.9	100.0	0.806	field_3	90.2	100.0	0.890
<b>2 (2 fx)</b>				field_4	92.2	100.0	0.888
field_1	40.8	97.6	0.330	field_5	82.5	96.3	<b>0.007</b>
field_2	43.4	99.7	0.771	field_6	84.3	95.2	<b>0.011</b>
field_3	70.1	100.0	0.967	field_7	82.2	96.2	<b>0.008</b>
<b>3 (2 fx)</b>				field_8	81.2	95.4	<b>0.005</b>
field_1	99.9	100.0	1.000	<b>12 (2 fx)</b>			
field_2	99.4	100.0	0.754	field_1	96.5	100.0	0.808
field_3	98.7	100.0	0.890	field_2	96.1	100.0	0.694
<b>4 (2 fx)</b>				field_3	93.1	100.0	0.655
field_1	100.0	100.0	0.890	<b>13 (2 fx)</b>			
field_2	99.9	100.0	0.751	field_1	99.4	100.0	0.736
field_3	100.0	100.0	0.961	field_2	99.6	100.0	0.888
field_4	100.0	100.0	0.888	field_3	98.6	100.0	0.888
<b>5 (2 fx)</b>				field_4	99.3	100.0	0.838
field_1	99.9	100.0	0.888	<b>14 (2 fx)</b>			
field_2	99.9	100.0	0.888	field_1	99.6	100.0	0.909
<b>6 (2 fx)</b>				field_2	99.7	100.0	0.288
field_1	69.3	88.1	<b>0.001</b>	field_3	99.7	100.0	0.669
field_2	69.6	88.3	<b>0.005</b>	field_4	99.7	100.0	0.874
field_3	72.0	88.6	<b>0.001</b>	<b>15 (3 fx)</b>			
<b>7 (2 fx)</b>				field_1 2->1	98.8	100.0	0.899
field_1	99.4	100.0	0.870	field_1 3->2	97.8	100.0	0.792
field_2	98.6	100.0	0.891	field_2 2->1	98.6	100.0	0.794
field_3	99.7	100.0	0.885	field_3 3->2	92.0	98.3	0.944
field_4	99.5	100.0	0.871	field_3 2->1	98.4	100.0	0.888
field_5	99.5	100.0	0.891	field_3 3->2	97.9	100.0	0.791
field_6	99.7	100.0	0.867	<b>16 (2 fx)</b>			
<b>8 (3 fx)</b>				field_1	88.8	99.6	0.625
field_7 2->1	99.7	100.0	0.885	field_2	88.5	99.3	0.398
field_7 3->1	99.8	100.0	0.873	field_3	95.2	99.9	0.786
field_8 2->1	100.0	100.0	0.895	field_4	95.6	99.2	0.431
field_8 3->1	99.2	100.0	0.884	<b>17 (2 fx)</b>			
field_9 2->1	99.7	100.0	0.896	field_1	99.2	100.0	0.624
field_9 3->1	99.8	100.0	0.876	field_2	98.5	100.0	0.817
field_10 2->1	99.3	100.0	0.890	field_3	99.1	100.0	0.888
field_10 3->1	99.9	100.0	0.895	field_4	99.0	100.0	0.798
field_11 2->1	99.6	100.0	0.875	field_5	98.8	100.0	0.888
field_11 3->1	99.7	100.0	0.884	<b>18 (2 fx)</b>			
field_12 2->1	100.0	100.0	0.873	field_1	98.9	100.0	0.988
field_12 3->1	99.0	100.0	0.891	field_2	99.0	100.0	0.931
<b>9 (2 fx)</b>				field_3	98.8	100.0	0.745
field_5	88.9	96.8	0.888	field_4	98.6	100.0	0.687
field_6	89.6	97.5	<b>0.021</b>	field_5	99.5	100.0	0.735
<b>10 (3 fx)</b>				<b>19 (2 fx)</b>			
field_1 2->1	49.1	92.6	<b>0.012</b>	field_1	50.7	100.0	0.882
field_1 3->1	66.7	92.2	<b>0.006</b>	field_2	47.3	100.0	0.992
field_2 2->1	48.4	92.1	<b>0.009</b>	field_3	48.8	100.0	0.888
field_2 3->1	64.3	91.3	<b>0.000</b>	field_4	46.0	100.0	0.830
field_3 2->1	39.7	90.5	<b>0.046</b>				
field_3 3->1	53.3	88.5	<b>0.006</b>				

An alternative method of dose measurement can be usage of external detector matrix and dose reconstruction software [28,29]. This processing can be made to assess the compliance of the calculated and delivered dose. Nevertheless, almost every biomedical accelerator (C-arm type) is equipped with EPID array which is an integral element of modern therapeutic units. Thus in the present work the EPID matrix was used.

This work is an attempt to present a method of using the EPID matrix for the measurements of dose and geometry changes. At this point it should be highlighted that in present work the measured dose is not compared with the dose calculated in treatment planning system. The proposed method allows fluence maps measuring in subsequent sessions with the presence of the patient and comparing them with the reference one. It is recommended to utilize the fluence map acquired for the first fraction as the reference data set. As before the required step is patient position verification before each session.

The measurements confirm that simulated dose change causes the expected change in the measured maps. It should be noted, that the displacement of structures relative to the planned position also causes differences in measured fluence maps. It can also be stated that the arrays of the aS1200 EPID detectors are very stable measuring matrices, with a measurement uncertainty of 1.1%.

This work is not about the agreement between measured and calculated dose, but about the repeatability of measurements. The EPID arrays show the linearity of the read signal with the radiation dose. In the tested dose range from 0.5 to 7.0 Gy, the R2 correlation coefficient is equal to one. Analysis of clinical cases indicates that repetitive dose was delivered to the patients undergoing radiosurgical treatment and no shifts in the irradiated area were detected.

Radiosurgical patients are very precisely immobilized so mobility during the therapeutic session is negligible. This is confirmed by imaging performed during each therapeutic session with the OBI device. The proposed method can be used to assess the repeatability of radiation therapy, both in assessing the value of the delivered dose and its location. The further test of the method will be continued for fractionated radiotherapy and with extracranial locations.

## Conclusions

The performed measurements, calculations, and analysis indicate that the EPID detector matrix can be used for dosimetric and geometric QC in dynamic stereotactic radiation therapy. This technique could be applied both for dose and geometric changes among treatment sessions.

## References

- [1] Herman MG, Balter JM, Jaffray DA, et al. Clinical use of electronic portal imaging: Report of AAPM Radiation Therapy Committee Task Group 58. *Med Phys.* 2001;28(5):712-737.
- [2] Herman MG, Kruse JJ, Hagness CR. Guide to clinical use of electronic portal imaging. *J Appl Clin Med Phys.* 2000;1(2):38-57.
- [3] Bogaerts R, Van Esch A, Reymen R, Huyskens D. A method to estimate the transit dose on the beam axis for verification of dose delivery with portal images. *Radiother Oncol.* 2000;54(1):39-46.
- [4] Pasma KL, Kroonwijk M, Quint S, et al. Transit dosimetry with an electronic portal imaging device (EPID) for 115 prostate cancer patients. *Int J Radiat Oncol Biol Phys.* 1999;45(5):1297-1303.
- [5] Kroonwijk M, Pasma KL, Quint S, et al. In vivo dosimetry for prostate cancer patients using an electronic portal imaging device (EPID); demonstration of internal organ motion. *Radiother Oncol.* 1998;49(2):125-132.
- [6] Huyskens D, Van Dam J, Dutreix A. Midplane dose determination using in vivo dose measurements in combination with portal imaging. *Phys Med Biol.* 1994;39(7):1089-1101.
- [7] Woźniak B, Ganowicz M, Bekman A, Maniakowski Z. A comparison of the dosimetric properties of The Electronic Portal Imaging Devices (EPIDs) LC250 and aS500. *Rep Pract Oncol Radiother.* 2005;10(5):249-254.
- [8] Ganowicz M, Woźniak B, Bekman A, Maniakowski Z. Using an electronic portal imaging device for exit dose measurements in radiotherapy. *Nowotwory J Oncol.* 2003;53(6):626-629.
- [9] Ding GX, Munro P. Comparing MV And kV Imaging Doses For Image Guided Radiation Therapy. *Proceedings of the 53rd Annual ASTRO Meeting. Int J Radiat Oncol Biol Phys.* 2011;81(2 Supp):S771-S772
- [10] Boas FE, Fleischmann D. CT artifacts: Causes and reduction techniques. *Imaging Med.* 2012;4(2):229-240.
- [11] Li H, Noel C, Chen H, et al. Clinical evaluation of a commercial orthopedic metal artifact reduction tool for CT simulations in radiation therapy. *Med Phys.* 2012;39(12):7507-7517.
- [12] Boas FE, Fleischmann D. Evaluation of Two Iterative Techniques for Reducing Metal Artifacts in Computed Tomography. *Radiology.* 2011;259(3):894-902.
- [13] van Zijtveld M, Dirx ML, de Boer HC, Heijmen BJ. Dosimetric pre-treatment verification of IMRT using an EPID; clinical experience. *Radiother Oncol.* 2006;81(2):168-175.



- [14] Wendling M, Louwe RJ, McDermott LN, et al. Accurate two-dimensional IMRT verification using a back-projection EPID dosimetry method. *Med Phys*. 2006;33(2):259-273.
- [15] McDermott LN, Wendling M, Sonke JJ, et al. Replacing pretreatment verification with in vivo EPID dosimetry for prostate IMRT. *Int J Radiat Oncol Biol Phys*. 2007;67(5):1568-1577.
- [16] McDermott LN, Wendling M, Nijkamp J, et al. 3D in vivo dose verification of entire hypo-fractionated IMRT treatments using an EPID and cone-beam CT. *Radiother Oncol*. 2008;86(1):35-42.
- [17] van Elmpt W, Nijsten S, Mijnheer B, et al. The next step in patient-specific QA: 3D dose verification of conformal and intensity-modulated RT based on EPID dosimetry and Monte Carlo dose calculations. *Radiother Oncol*. 2008;86(1):86-92.
- [18] van Elmpt W, Nijsten S, Petit S, et al. 3D in vivo dosimetry using megavoltage, cone-beam CT and EPID dosimetry. *Int J Radiat Oncol Biol Phys*. 2009;73(5):1580-1587.
- [19] van Elmpt W, Petit S, De Ruyscher D, et al. 3D dose delivery verification using repeated cone-beam imaging and EPID dosimetry for stereotactic body radiotherapy of non-small cells lung cancer. *Radiother Oncol*. 2010;94(2):188-194.
- [20] Mijnheer B, Olaciregui-Ruiz I, Rozendaal R, et al. 3D EPID – based in vivo dosimetry for IMRT and VMAT. *J Phys: Conf Series*. 2013;444:012011.
- [21] van Zijtveld M, Dirkx ML, de Boer HC, Heijmen BJ. 3D dose reconstruction for clinical evaluation of IMRT pretreatment verification with an EPID. *Radiother Oncol*. 2017;82(2):201-207.
- [22] TRUEBEAM STx System Specifications. Available at : [varian.com](http://varian.com).
- [23] Eclipse Photon and Electron Algorithms Reference Guide, P1008611-002-B, Varian Medical Systems (September 2014).
- [24] Portal Dosimetry Reference Guide, P1001364B, Varian Medical Systems (2013).
- [25] Low DA, Harms WB, Mutic S, Purdy JA. A technique for the quantitative evaluation of dose distributions. *Med Phys*. 1998;25(5):656-661.
- [26] Slosarek K, Szlach M, Bekman B, Grzadziel A. EPID in vivo dosimetry in RapidArc technique. *Rep Pract Oncol Radiother*. 2010;15(1):8-14.
- [27] Fidanzio A, Cilla S, Greco F, et al. Generalized EPID calibration for in vivo transit dosimetry. *Phys Med*. 2011;27(1):30-38.
- [28] Valve A, Keyriläinen J, Kulmala J. Compass model-based quality assurance for stereotactic VMAT treatment plans. *Phys Med*. 2017;44:42-50.
- [29] Nakaguchi Y, Ono T, Maruyama M, et al. Validation of a method for in vivo 3D dose reconstruction in SBRT using a new transmission detector. *J Appl Clin Med Phys*. 2017;18(4):69-75.